

## Adsorption of Basic Violet 16 dye from aqueous solution onto mucilaginous seeds of *Salvia sclarea*: kinetics and isotherms studies

Shirin Afshin<sup>a,b</sup>, Yousef Rashtbari<sup>a,b</sup>, Mohammad Shirmardi<sup>c,d</sup>, Mehdi Vosoughi<sup>b,e,\*</sup>, Asghar Hamzehzadeh<sup>a</sup>

<sup>a</sup>Students Research Committee, Ardabil University of Medical Sciences, Ardabil, Iran, Tel. +98 9014515339; email: shirinafshin1990@gmail.com (S. Afshin), Tel. +989383162079; email: u3f.rashtbari@gmail.com (Y. Rashtbari), Tel. +98 9143540015; email: a.hamzezade@yahoo.com (A. Hamzehzadeh)

<sup>b</sup>Department of Environmental Health Engineering, School of Public Health, Ardabil University of Medical Sciences, Ardabil, Iran, Tel. +989120910243; email: mvn\_20@yahoo.com

<sup>c</sup>Environmental Health Research Center, Health Research Institute, Babol University of Medical Sciences, Babol, Iran, Tel. +989362173856; email: mohammadshirmardi@yahoo.com

<sup>d</sup>Department of Environmental Health Engineering, Faculty of Paramedical Sciences, Babol University of Medical Sciences, Babol, Iran

<sup>e</sup>Social Determinants of Health Research Center, Ardabil University of Medical Sciences, Ardabil, Iran

Received 18 October 2018; Accepted 13 April 2019

### ABSTRACT

The *Salvia sclarea* seeds (SSS) were used as adsorbent for the removal of Basic Violet 16 (BV 16) dye from aqueous solutions. The structure and surface characteristics of the SSS were investigated by field emission scanning electron microscopy, Fourier transform infrared spectroscopy, Brunauer–Emmett–Teller and pH point of zero charge ( $\text{pH}_{\text{pzc}}$ ) procedures. The effect of SSS dosage, pH of the solution, contact time and initial concentration of BV 16 dye on its removal was elucidated. The experimental data were analyzed by the Langmuir, Freundlich and Temkin isotherm models. The adsorption isotherm data were fitted well to Langmuir isotherm and the monolayer adsorption capacity was found to be 19.80 mg/g. The kinetic data obtained at different concentrations have been analyzed using a pseudo-first-order, pseudo-second-order equation. The kinetic studies showed that the pseudo-second-order kinetic model better described the adsorption of BV 16 dye onto the SSS. The findings reveal the feasibility of the SSS to be used as a potential and low-cost adsorbent in water and wastewater industry for the removal of various pollutants, more specifically cationic dyes.

**Keywords:** Adsorption; *Salvia sclarea* seeds; Basic Violet 16; Isotherm; Kinetics

### 1. Introduction

In recent years, with the increase in population and development of various industries, the utilization, and subsequently discharge of wastewater containing dyes into the environment has increased. Discharge of textile effluent to receiving water sources without treatment is considered

as one of the major issues of global concern [1–3]. The presence of even a very low concentration of any kinds of dyes in the effluents is quite visible and undesirable [4]. Low concentration of dyes can disturb the photosynthesis in water media due to the reduction of light penetration [5]. Basic Violet 16 (BV 16) is a cationic dye, highly water soluble and nonvolatile [6,7]. It is a toxic substance and may

\* Corresponding author.

have adverse effects on body systems such as skin, eyes and gastrointestinal tract. Its carcinogenicity and toxicity toward humans and animals have also been experimentally proven [8]. It is widely used in textile, leather industries and is also a well-known water tracer fluorescent [7]. Various methods such as chemical oxidation [9,10], ozonation [11], aerobic and anaerobic microbial degradation [12], coagulation–flocculation [13] and membrane process [14] were used for removal of dyes. The mentioned processes have many disadvantages such as high reagents and energy requirements and generation of toxic sludge which again needs safe disposal [15]. On the other hand, the adsorption processes have been reported as an alternative method for removal of a wide range of dyes [16]. The low cost, simplicity of design, high removal efficiency, insensitivity to toxic substances and simple operation make adsorption a suitable technology for the removal of organic pollutants such as dyes [17]. Many researchers have used natural materials as adsorbent for removal of aqueous pollutants; however, they have not used mucilage properties for this aim. Lakshmanraj et al. [15] reported the use of boiled seeds of *Ocimum americanum* to biosorption of hexavalent chromium from aqueous solutions and the biosorption capacity calculated  $q_m = 32$  mg/g. Pavan et al. [18] studied the biosorption of a crystal violet dye from aqueous phase onto *Formosa papaya* seed powder and the maximum adsorption capacity obtained by the Langmuir model was 85.99 mg/g. The removal of cationic dye from aqueous solutions using citric acid esterifying wheat straw in  $q_m = 227.27$  mg/g has been obtained by Gong et al. [19]. These kinds of adsorbents have significant characteristics that are desirable for the adsorption process such as high adsorption capacity, low-cost preparation and high possibility of regeneration [18]. Organic adsorbents are biodegradable and safer for human health. The genus *Salvia* is a member of the mint family, Lamiaceae, and is the largest genus in that family [20]. The novelty of this study is the usage of mucilage polysaccharide for adsorption of pollutants. *Salvia sclarea* seeds become gelatinous when soaked in water due to its high mucilage content. The mucilaginous seeds can be used as a novel source of food hydrocolloid [21]. The mucilaginous seeds of hydrocolloids are used as a substitution to the conventional ones as a thickening agent, fat replacer and stabilizer for the development of novel food/cosmetic formulations [20]. In result, polysaccharide and protein available in seeds and its powder are both nontoxic and biodegradable that can be advocated as a sustainable technology for water treatment [22]. The researchers reported the use of synthetic polysaccharide as adsorbents in few literatures; however, we could not find the use of mucilage of seeds such as *Salvia sclarea* as an interesting and novel adsorbent for the removal of aqueous pollutants. The main objective of this study was to investigate *Salvia sclarea* seeds for adsorption of Basic violet 16 dyes as eco-friendly adsorbents.

## 2. Materials and methods

### 2.1. Reagents, materials and solutions

The Basic Violet 16 dye used in this study was purchased from Alvan Sabet Co., Hamedan, Iran. Physico-chemical

properties of the BV 16 dye are given in Table 1, and were used without further purification. Other Chemicals used in the experiments were obtained from Merck Chemical Co., Germany. The pH of the solution was adjusted by 0.1 M  $H_2SO_4$  or NaOH if necessary. A stock solution of 1,000 mg/L was prepared by dissolving the required quantity of the dye in distilled water. Deionized water was used in all experiments for dilution.

### 2.2. Preparation of *Salvia sclarea* seeds

*Salvia sclarea* seeds (SSS) were obtained from the local grocery in Ardabil, Iran. The seeds were cleaned manually to remove all foreign matter such as dust, dirt, stones and chaff. No other chemical or physical treatments were applied before adsorption experiments.

### 2.3. Adsorption experiments

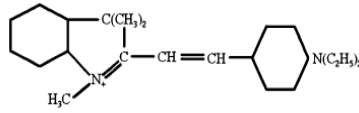
Adsorption experiments were conducted using a batch technique. The laboratory parameters for the study were pH (4–11), adsorbent dosage (2.5–17.5 g/L), the initial concentration of dye (10–100 mg/L) and contact time (5–220 min). For the study of the kinetics of adsorption, a series of 250 mL Erlenmeyer flasks were provided with dye solution of varying concentrations. After adjusting the pH, the appropriate amount of the adsorbent was added to the solution. The solutions were agitated for achieving equilibrium time at room temperature at a constant speed (250 rpm). After reaching equilibrium adsorption time, the adsorbent was separated from the solution by using a centrifuge machine at 4,000 rpm for 3 min. The remaining concentration of the dye in the solution was analyzed using a UV–visible spectrophotometer. Isotherm and kinetic studies were carried out by varying the initial concentration of dye solution in optimum conditions. After equilibrium, the removal efficiency and the adsorption capacity ( $q_e$ , mg/g) were calculated using Eqs. (1) and (2), respectively [23–25]:

$$\text{Removal Percentage (\%)} = \left( \frac{C_0 - C_e}{C_0} \right) \times 100 \quad (1)$$

$$\text{Adsorption capacity, } q_e = \frac{(C_0 - C_e) \times V}{M} \quad (2)$$

where  $C_0$  is the initial dye concentration (mg/L);  $C_e$  is the dye concentration at the time of equilibrium (mg/L);  $V$  is

Table 1  
Physico-chemical properties of dye Basic Violet 16

|                     |   |
|---------------------|---|
| Molecular structure |  |
| Molecular formula   | $C_{23}H_{29}ClN_2$   |
| Molecular weight    | 368.95 g/mol  |
| $\lambda_{max}$     | 545 nm  |

the volume of dye solution (L) and  $M$  is the dry weight of adsorbent used (g).

#### 2.4. Adsorption isotherms

In order to successfully represent the equilibrium adsorption behavior, it is essential to have a satisfactory description of the equation stating between the two phases of adsorbate and adsorbent. The adsorption isotherms were determined at room temperature and BV 16 concentration of 10, 25, 50, 75, 100, 150, 200, 250, and 300 mg/L in 100 mL solution with adding 10 g/L of the adsorbent. The isotherm experiment was conducted in a batch system in the optimal conditions and equilibrium time for dye removal. Three kinds of isotherm models (Langmuir, Freundlich and Temkin) were tested to fit the experimental data. Langmuir isotherm is represented as follows [26–29]:

$$\frac{1}{q_e} = \frac{1}{k_1 \times q_m \times C_e} + \frac{1}{q_m} \quad (3)$$

where  $q_e$  is the amount of BV 16 adsorbed per unit mass of the adsorbent at equilibrium (mg/g);  $q_m$  is the maximum adsorption capacity of the adsorbent (mg/g);  $k_1$  is the Langmuir constant (L/mg);  $C_e$  is the dye concentration in the solution at equilibrium (mg/L).

Freundlich isotherm is given as follows:

$$\log q_e = \log k_f + \frac{1}{n} \log C_e \quad (4)$$

$k_f$  is the Freundlich constant that is related to bond strength (mg/g) [mg/L]<sup>1/n</sup>;  $n$  is the Freundlich constant and indicative of bond energies between dye ions.

Temkin isotherm equation is given in a linearized form as [30,31] follows:

$$q_e = K_1 \ln K_2 + K_1 \ln C_e \quad (5)$$

$K_1$  is the Temkin isotherm energy constant (L/mol) and  $K_2$  is the Temkin isotherm constant.  $K_1$  and  $K_2$  could be calculated (Table 3) from the linear plot of  $\ln C_e$  against  $q_e$ .

The essential characteristics of the Langmuir isotherm are expressed in terms of a dimensionless constant named equilibrium parameter  $R_L$  that is indicative of the isotherm shape that predicts whether an adsorption system is favorable or unfavorable.  $R_L$  is defined as [32] follows:

$$R_L = \frac{1}{1 + k_L \times C_0} \quad (6)$$

The value of  $R_L$  indicates the type of isotherm to be favorable adsorption ( $0 < R_L < 1$ ), unfavorable ( $R_L > 1$ ), linear adsorption ( $R_L = 1$ ) or irreversible adsorption ( $R_L = 0$ ).

#### 2.5. Kinetic studies

Kinetic models were used to fit and evaluate the test experimental data corresponding to the adsorption of BV

16 onto SSS. In order to analyze the adsorption kinetics of dye, the pseudo-first-order and pseudo-second-order kinetic models were applied. The linear form of the pseudo-first-order equation is given as follows [33]:

$$\log (q_e - q_t) = \log q_e - \left( \frac{k_1}{2.303} \right) \times t \quad (7)$$

where  $q_t$  and  $q_e$  are the sorption capacity at any time  $t$  and equilibrium (mg/g), respectively, and  $k_1$  is the rate constant of this equation (1/min). The linear form of the pseudo-second-order rate equation is expressed as follows [34]:

$$\frac{t}{q_t} = \frac{1}{(k_2 q_e^2)} + \left( \frac{t}{q_e} \right) \quad (8)$$

where  $k_2$  is the rate constant of this equation (g/mg.min).

#### 2.6. Instruments

The remaining concentration of the BV 16 was analyzed by measuring the absorbance values after each experiment with a UV–Vis spectrophotometer (model DR 5000, HACH, USA) at 545 nm [35]. The morphology analysis of this SSS was carried out by scanning (Czech) under an acceleration voltage of 10 kV, and Fourier transform infrared spectroscopy (USA). For FTIR measurements, the SSS were prepared by using potassium bromide (KBr) as reference and analyzed with 1/cm resolution in a wide range of frequency 450–4,000 1/cm. The nitrogen adsorption/desorption isotherms were conducted by BET analysis (Japan) at 77 K to determine the pore volume and specific surface area of the SSS.

### 3. Results and discussion

#### 3.1. Characteristics of the adsorbent

##### 3.1.1. Determination of $\text{pH}_{\text{pzc}}$

The experiments related to pH zero point of charge ( $\text{pH}_{\text{pzc}}$ ) of the SSS was performed at pH range 4–11. At first, 100 mL of aqueous solution was transferred to a series of Erlenmeyer flasks and then pH was adjusted to desirable values by adding a few drops of 0.1 M  $\text{H}_2\text{SO}_4$  or 0.1 M NaOH solutions. After that 3 g of SSS was added to each flask and the final pH was measured after 48 h under agitation at room temperature. The initial values ( $\text{pH}_i$ ) vs. the final pH ( $\text{pH}_f$ ) were plotted. The  $\text{pH}_{\text{pzc}}$  is the point of intersection of the resulting curve at which  $\text{pH} = 6.93$  [18].

##### 3.1.2. FTIR analysis

FTIR spectroscopy provides structural and compositional information on the functional groups presented in the samples. The proximate composition of the SSS was investigated by Fourier transform infrared (FTIR) spectroscopy. Fig. 1 indicates the FTIR spectrum of the SSS adsorbent. As shown in the figure, the spectrum displays some absorption peaks, indicating the simple nature of

the SSS. The FTIR spectrum of SSS shows that the peak positions are at 3,436; 2,924 and 1,640  $\text{cm}^{-1}$ . The peaks at 3,436 and 2,924  $\text{cm}^{-1}$  are due to  $-\text{OH}$  stretching and  $\text{C}-\text{H}$  is stretching, respectively. The peak value at 1,640  $\text{cm}^{-1}$  confirms the functional groups  $\text{C}=\text{O}$  bending [21,36]. Mechanism of dye removal by seeds follows the mechanism of adsorption. When the mucilage happens around the outer layer of seed, the natural polysaccharide extends in aqueous solution and can contact with pollutant molecules. According to the FTIR results several dominant functional groups play significant role in adsorption of dye with mucilage phenomena. The surface of SSS has the functional group of  $\text{C}-\text{H}$  and  $\text{C}=\text{O}$  as dominant bend. The carboxyl group existing in dye structure reacts with functional groups of seed.

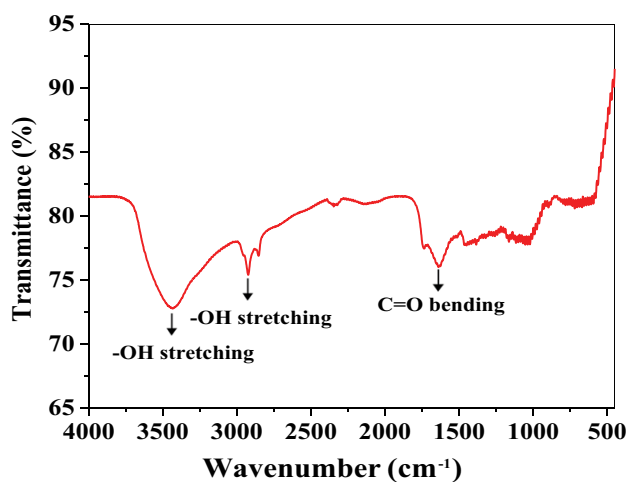


Fig. 1. FTIR of *Salvia sclarea* seeds before dye adsorption.

### 3.1.3. FESEM analysis

Field emission scanning electron micrograph (FESEM) images of adsorbent clearly indicate the surface prominent textures of the *Salvia sclarea* seed in Fig. 2. Textures being the prominent component indicate the mucilaginous nature which in turn adsorbs the BV 16 dye. Textures of surface seem to be relatively smooth, however the seed comprises a thin layer having larger capacity of hydration in outer side of surface. After soaking in water, the outer layer of seeds swells which seems as a white gel named as mucilage. When the seeds were soaked in water, they swell and absorb more water.

### 3.1.4. BET analysis

The pore structures of SSS were studied by  $\text{N}_2$  adsorption/desorption analysis (Fig. 3). Surface area of SSS was observed 3.05  $\text{m}^2/\text{g}$ . The results of BET analysis (Fig. 3 and Table 2) showed that the surface area of seed is lower compared with other adsorbents such as activated carbon. This predictable result implies that the surface area of seed is not a significant parameter for adsorption of dye. As provided in Fig. 5, the main reason of adsorption of dye by seed is mucilage as a natural polysaccharide. The surface of seed extends their polysaccharide when contact with the water. Therefore, this polysaccharide of seed adsorbs the dye molecule.

## 3.2. Removal properties of BV 16

### 3.2.1. Effect of the initial pH

The pH of the solution may influence the functional groups present on the surface of the adsorbent and may determine the solubility of the dyes in aqueous solutions. The results for the effect of the initial pH of the solution

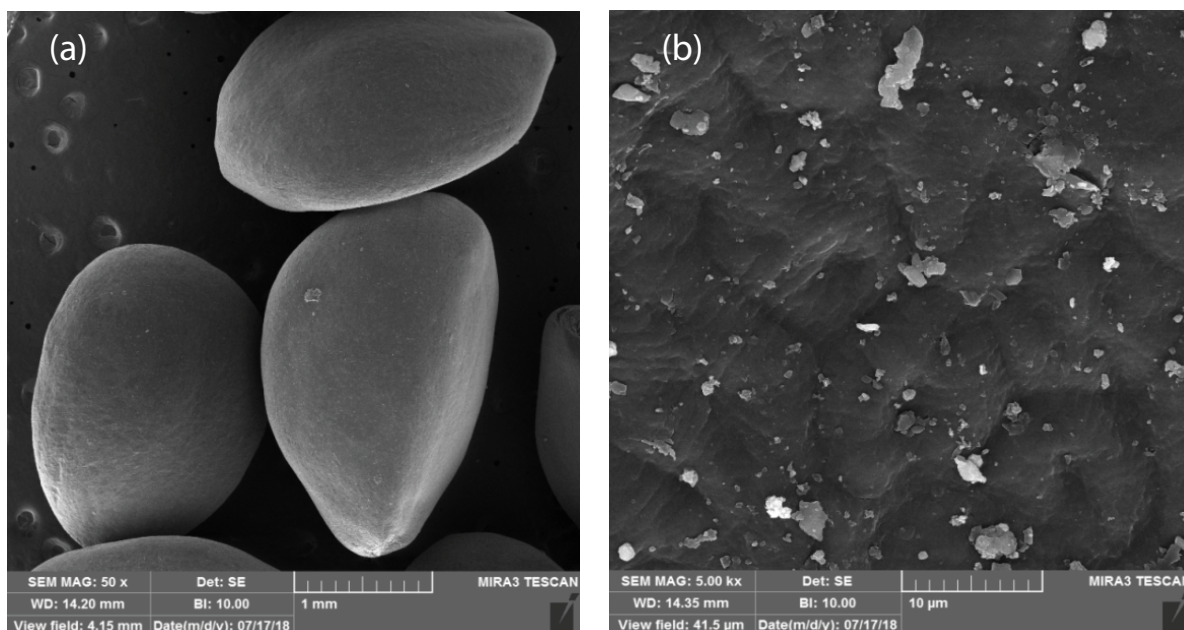


Fig. 2. FESEM images for *Salvia sclarea* seeds before dye adsorption. (a) FESEM images for *Salvia sclarea* seeds with size of 1 mm and (b) FESEM images for surface of *Salvia sclarea* seeds with size of 10  $\mu\text{m}$ .

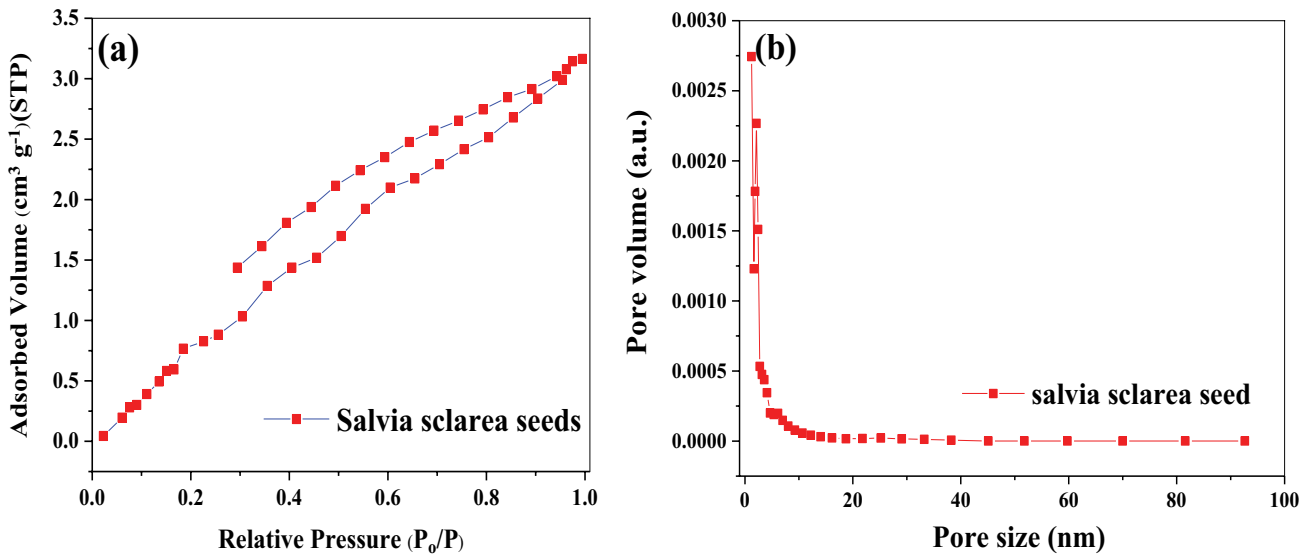


Fig. 3. Nitrogen adsorption isotherms of SSS at 77 K (a) and the pore size distribution (b).

Table 2

Specific surface area ( $S_{BET}$ ), total pore volume ( $V_{Total}$ ) and mean pore diameter ( $D_p$ ) of SSS

| Material | $S_{BET}$ (m²/g) | $V_{Total}$ (cm³/g) | $D_p$  |
|----------|------------------|---------------------|--------|
| SSS      | 3.0532           | 0.0048852           | 6.4002 |

on the adsorption capacity of the BV 16 dye on the SSS are presented in Fig. 4. The figure shows that as the pH value is increased from 4 to 7, an increase in the BV 16 removal percentage occurred from 29.2% to 40.2% (Fig. 4a). In the pH range of 8–11, the BV 16 dye removal changes are not remarkable compared with pH of 7. This shows that the optimal pH for the adsorption of BV 16 by SSS is neutral pH = 7.

At pH 7, the highest removal percentage was obtained, and the lowest residual dye concentrations remained in the solution. Similar results were obtained by Mahmoodi et al. [35]. They found that pH 8 was the optimum pH in the removal of the BV 16 dye using biopolymer [35]. The point of zero charge ( $pH_{pzc}$ ) of the SSS could be used to explain the influence of pH (Fig. 4b). The  $pH_{pzc}$  of the SSS was found to be 6.93. Therefore, at pH values lower than 6.93 ( $pH < pH_{pzc}$ ), the surface of the SSS is positively charged, inhibiting the adsorption of cationic dye due to the electrostatic repulsion between the cationic structure of BV 16 dye and the SSS. On the other hand, at pH values above 6.93 ( $pH > pH_{pzc}$ ) the surface of SSS was negatively charged, facilitating the electrostatic attraction between the cationic dye and adsorbent, and consequently, increasing the BV 16 dye removal percentage. However, this increase is not remarkable at higher pH.

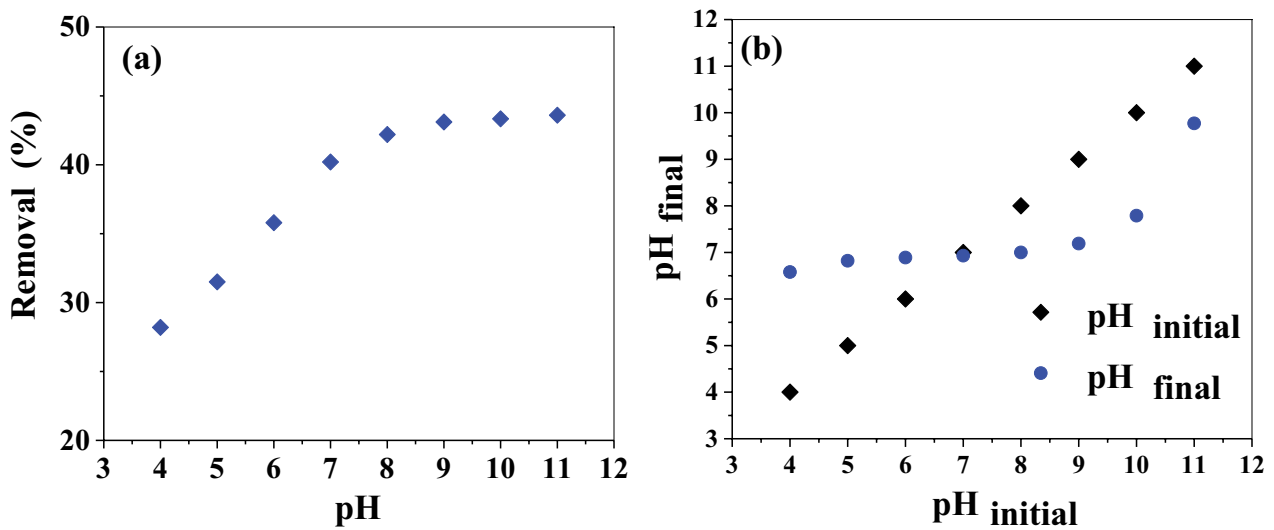


Fig. 4. Effect of initial pH (a) and  $pH_{pzc}$  (b) (initial dye concentration: 50 mg/L; SSS dosage: 5 g/L; contact time: 60 min).



The chemical properties of the adsorbent surface can be used to measure its ability to remove pollutants from aqueous solutions. The SSS adsorbent has the advantage of having several functional groups on its surface, such as hydroxyl and carboxyl groups. Surface functional groups are available on the surface of the adsorbent to attract the cationic groups of the dye molecules. El-Sayed [31] determined that the effective adsorption of the crystal violet dye with palm kernel fiber was obtained at pH 7.2. They reported that this result can be attributed to the presence of negatively charged functional groups such as  $\text{OH}^-$  on the palm kernel fiber structure [31]. Also, our results are in agreement with those reported by Sartape et al. [36] who found that the removal of cationic dye by *Limonia acidissima* shell was maximal at pH 7.5–8. More recently, Katal et al. [37] also reported that the removal of cationic dye by neem sawdust was maximal at pH 7.

### 3.2.2. Effect of adsorbent dosage

The effect of SSS dosage on the adsorption process was studied by changing the sorbent dosage from 2.5 to 17.5 g/L

of BV 16 solution. The effects of SSS dosage on the uptake ratios of dyes are shown in Fig. 5a. When the SSS dosage is increased, the efficiency of dye adsorbed increases from 25.8% to 52.3%. As shown in Fig. 5a, for the adsorbent dosage higher than 10 g/L, there is no significant increase in adsorption. Therefore, the SSS dosage of 10 g/L was chosen for the next experiments.

As shown in Fig. 1, the surface of the SSS has hydroxyl ions. By increasing the amount of SSS, the number of available hydroxyls and carboxyl groups increase in the surface of seed and consequently, the removal of BV 16 dye with more intensity increases. On the other hand, increasing the percentage of dye removal by increasing the amount of adsorbent is justifiable by increasing access to active vacant sites [37]. At lower amounts of the adsorbent, there are fewer active sites available to dye molecules, which reduce the removal efficiency. Contrast to the removal efficiency with the increase in the amount of adsorbent dosage (g/L), the amount of adsorbed dye per unit mass of the adsorbent ( $q_e$ ) decreases. This phenomenon can be explained by the presence of more unsaturated sites on the adsorbent surface. These results are consistent with the findings by Gupta et al. [38] who have

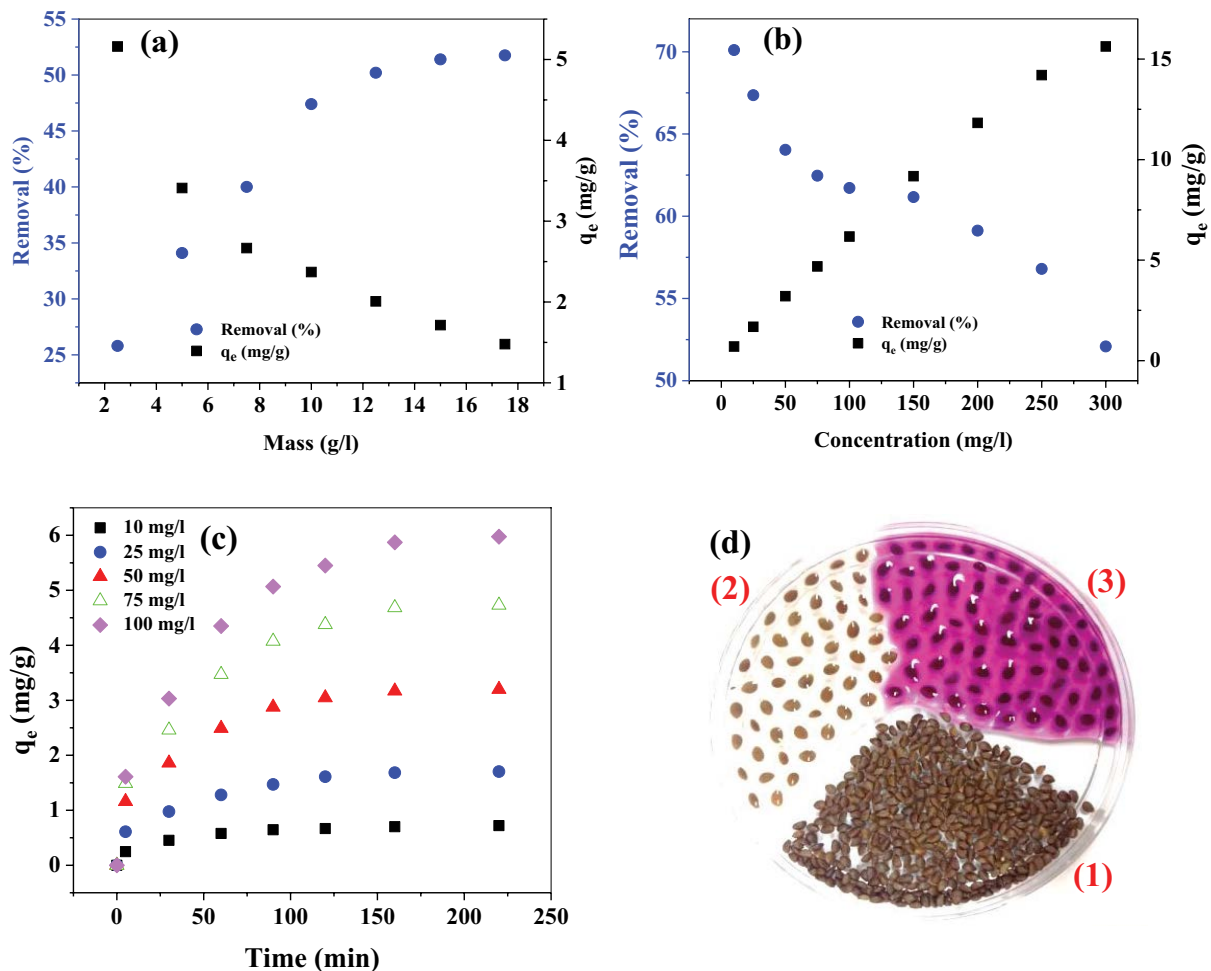


Fig. 5. (a) Effect of adsorbent dosage (contact time: 60 min, pH 7, initial dye concentration: 50 mg/L), (b) initial dye concentration (contact time: 180 min, pH: 7, adsorbent dosage: 10 g/L), (c) contact time (pH: 7, adsorbent dosage: 10 g/L) and (d) the image view of the *Salvia sclarea* seeds.

studied the removal of dye using activated carbon. Also, the similar mechanism for the adsorption of Congo red by jujuba seeds was previously reported [39].

### 3.2.3. Effect of initial BV 16 dye concentration on its adsorption by SSS

The effect of initial dye concentration on dye removal was studied. Experiments were conducted at different dye concentrations of 10–300 mg/L, 10 g/L of SSS, pH 7 and the agitation speed of 250 rpm at room temperature. Fig. 5b shows a direct relationship between the initial dye concentration with the adsorption capacity values ( $q_e$ ) and removal efficiency. As can be seen in Fig. 5b, the adsorption capacity values increased from 0.701 to 15.625 mg/g by increasing the dye concentration from 10 to 300 mg/L. The increase in the adsorption capacity values ( $q_e$ ) is maybe due to the greater interaction between the adsorbate and adsorbent at higher concentration of dye; it can be due to the increase in the driving force of the dye molecules toward adsorbent [15]. At the lower dye concentrations, the ratio of an initial number of dye molecules to the available adsorption sites is low. Also, the higher quantity of dye adsorption at higher concentrations is due to increased diffusion of dye on the adsorbent surface. Similar findings have also been reported by the other researchers [15,40–42]. Fig. 5d shows the image of the *Salvia sclarea* seeds (1), seeds soaked in water (2) and seeds soaked in water after adsorption (3).

### 3.2.4. Effect of contact time

The adsorption of BV 16 on SSS was studied at different BV 16 concentrations (10–100 mg/L). As shown in Fig. 5c, the removal percentage gradually increases with time until reaching equilibrium at 160 min. At all dye concentrations, the adsorption by SSS is slow and reaches equilibrium slowly. It indicates that the formation of mucilage layers on the surface of the SSS adsorbent is slow. As the contact time increases, the opportunity of the contact of dye molecules with the surface of the adsorbent increases and the amount of removal efficiency increases. The remaining constant amount of dye in solution at equilibrium time may be due to aggregation of dye molecules around the adsorbent particles that are saturated by the dye [43]. Lakshmanraj et al. [15] and Chakraborty et al. [44] studied and reported that the adsorption equilibrium of Cr(III) and cesium-137 and strontium-90 on boiled mucilaginous seeds of *Ocimum americanum* and seeds of *Ocimum basilicum* took 180 and 60 min, respectively.

### 3.2.5. Adsorption isotherms

Langmuir, Freundlich and Temkin isotherm models were used to study the adsorption behavior at different dye concentrations on SSS. The linearized Langmuir, Freundlich and Temkin isotherms of dye are shown in Figs. 6a–c. Results and regression coefficients were obtained using for three isotherm models and the results were consistent with the experimental data (Table 3). The Langmuir model provides parameters such as the  $k_L$  adsorption equilibrium constant, which is related to the adsorption free energy and corresponds to the affinity between the surface of the

adsorbent and adsorbate. As well as, the maximum adsorption capacity ( $q_{max}$ ), which is joined with the amount of dye adsorbed to complete a monolayer, or when all present sites have been filled, complete coverage is achieved [29]. Parameters derived from the Freundlich model, such as  $k_f$  and  $n$ , are related to the experimental constants in various environmental factors. In general, a suitable adsorbent has a value of  $n$  between 1 and 10. The high  $n$  value indicates the strong interaction between adsorption and absorption [29]. Temkin isotherm assumes that the heat of adsorption shows a linear decrease with coverage due to adsorbent–adsorbate interactions [5]. The values of  $q_{max}$  and  $k_L$  in the Langmuir model were found to be 19.8 mg/g and 0.012 L/mg, respectively. The value of the constants  $K_f$  and  $n$  in the Freundlich model was found to be 3.37 and 1.21, respectively. The value of Freundlich constant in the range of 1–10 indicates favorable adsorption. The values of  $n > 1.0$  represent favorable adsorption conditions, indicating the favorable adsorption of BV 16 onto SSS. The value of correlation coefficients obtained from Langmuir isotherm is  $R^2 = 0.9977$ , whereas Freundlich and Temkin isotherm models showed comparatively lower value  $R^2 = 0.9966$  and  $0.8776$ , respectively. Hence, Langmuir isotherm model gives better fit to the experimental data. In the present experiment, factor ( $R_L$ ) was found to be between 0.8918 and 0.2156, when the concentration of the dye was ranging between 10 and 300 mg/L. All the  $R_L$  values are presented in Fig. 5b indicate that the adsorption was favorable, and at high concentration, the adsorption is nearly irreversible. Mahmoodi et al. [35] reported a similar result for the adsorption of BV 16 by biopolymer, where results suggested that the Langmuir model has the best model to represent the dye adsorption isotherm. The maximum adsorption capacity of the dye on the SSS is about 19.8 mg/g, which is comparable with that of the adsorption abilities of some various biosorption on cationic dyes in Table 4.

### 3.2.6. Kinetic studies

For evaluating the adsorption kinetics of BV 16, the pseudo-first-order and pseudo-second-order kinetic models are used to fit the experimental data (Figs. 6c–d). The calculated and experimental parameters are shown in Table 4. The values of correlation coefficient in pseudo-second-order are high ( $R^2 = 0.9979$ ) and the theoretical  $q_{2,cal}$  values obtained, from this model are very closer to the experimental  $q_{e,exp}$  values at different initial BV 16 concentrations (Table 5). Also, the pseudo-first-order model, the correlation coefficient obtained in this study,  $R^2 = 0.8927$ , is lower compared with the correlation coefficient obtained from the pseudo-second order model. It implies that the overall rate of the adsorption process is controlled by chemisorption. The pseudo-second-order model suggests that the adsorption of BV 16 on SSS is a multi-step process, that is, involving sorption on the outer surface and diffusion into the adsorbent. This model suggests chemical sorption involving valence forces by sharing or exchange of electrons between the SSS and the BV 16 dye. For the adsorption of BV 16 onto SSS, the pseudo-second-order rate constant ( $k_2$ ) decreased from 0.0761 to 0.0053 g/mg min as the initial dye concentration was increased from 10 to 100 mg/L. Additionally, the values of  $q_{2,cal}$  at 10, 25, 50, 75 and 100 mg/L (0.77, 1.86, 3.52, 5.27 and

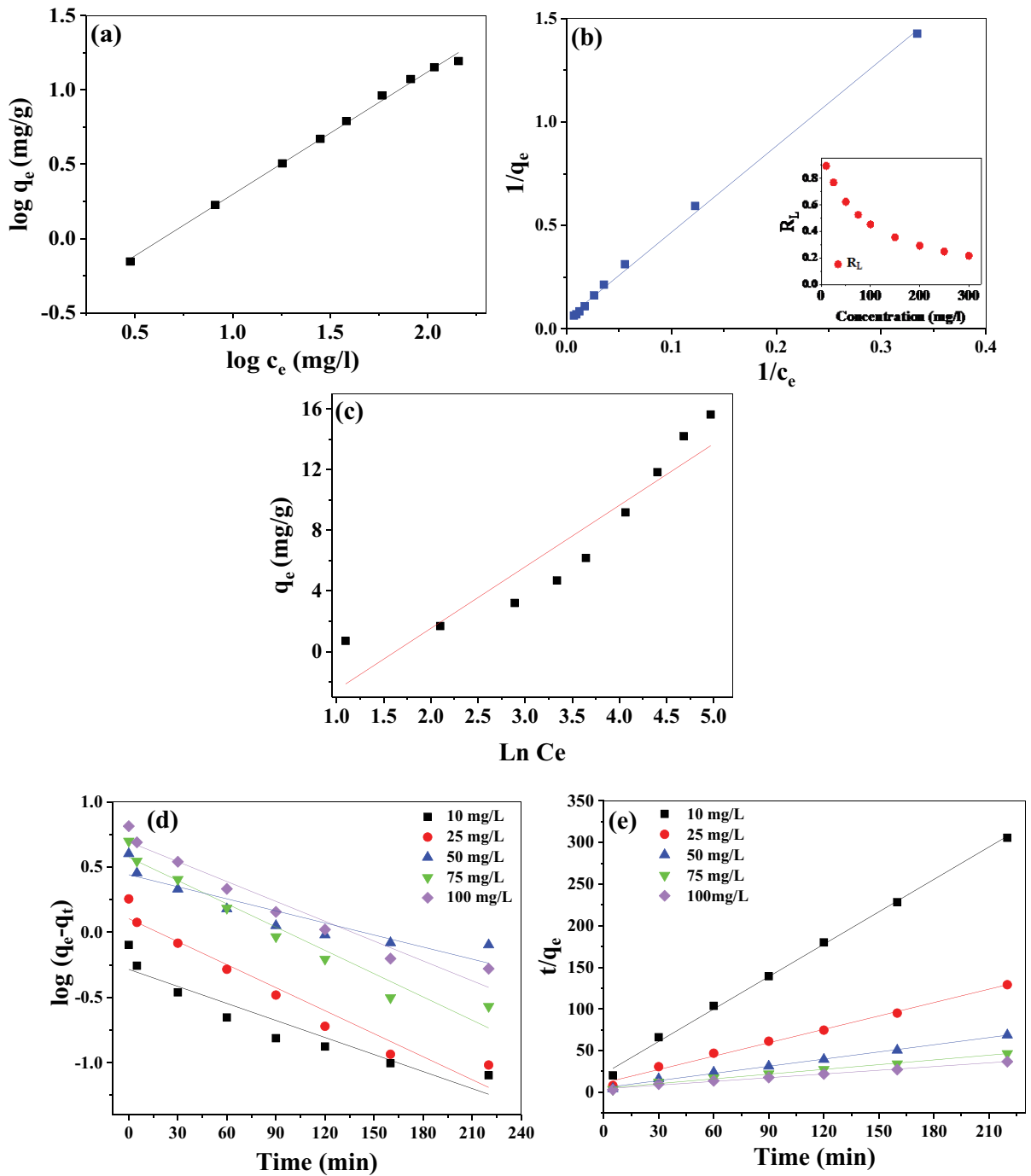


Fig. 6. Langmuir (a), Freundlich (b) isotherm and separation factor ( $R_L$ ) and Temkin (c) (pH 7; contact time: 180 min; SSS dosage: 10 g/L) and pseudo-first-order and (d) pseudo-second-order (e).

Table 3  
 Constants of adsorption isotherms of BV 16 on SSS

| Isotherm model | Langmuir isotherm |              |        |       | Freundlich isotherm                   |       |        | Temkin isotherm |       |        |
|----------------|-------------------|--------------|--------|-------|---------------------------------------|-------|--------|-----------------|-------|--------|
|                | $k_L$ (L/mg)      | $q_m$ (mg/g) | $R^2$  | $R_L$ | $k_f$ ([mg/g] [mg/L] <sup>1/n</sup> ) | $n$   | $R^2$  | A               | B     | $R^2$  |
| Value          | 0.0121            | 19.80        | 0.9977 | 0.215 | 3.378                                 | 1.211 | 0.9966 | 0.1975          | 4.056 | 0.8776 |



Table 4  
Comparison of the maximum adsorption capacities ( $q_{\max}$ ) of various adsorbents for cationic dyes

| Adsorbent                       | Dye             | pH    | Concentration (mg/L) | dosage (g/L) | Time (min) | $q_{\max}$ (mg/g) | Reference  |
|---------------------------------|-----------------|-------|----------------------|--------------|------------|-------------------|------------|
| <i>Limonia acidissima</i> shell | Malachite green | 7.5–8 | 100                  | 0.4          | 210        | 80.645            | [36]       |
| Neem sawdust                    | Malachite green | 7.2   | 12                   | 5            | 14         | 4.35              | [45]       |
| Cellulose powder                | Malachite green | 7.2   | 40                   | 5            | 30         | 2.422             | [46]       |
| Coir pith                       | Basic violet 10 | 8.6   |                      | 20           | 15         | 2.56              | [47]       |
| Grape seed                      | Crystal violet  | 6     | 5.5                  | 0.65         | 900        | -                 | [22]       |
| Palm kernel fiber               | Crystal violet  | 7     | 20                   | 2            | 60         | 78.9              | [31]       |
| Palm kernel fiber               | Methylene Blue  | 7     | 20                   | 2            | 60         | 95.4              | [31]       |
| Sugarcane dust                  | Crystal violet  | 7.5   | 8                    | 0.25         | 14         | 3.8               | [48]       |
| <i>Salvia sclarea</i> seeds     | Basic Violet 16 | 7     | 50                   | 10           | 160        | 19.80             | This study |

Table 5  
Rate constant at different concentration for adsorption of BV 16 on SSS

| $C_0$ (mg/L) | $q_{e, \text{exp}}$ (mg/g) | Pseudo-first-order         |               |         | Pseudo-second-order        |                  |        |
|--------------|----------------------------|----------------------------|---------------|---------|----------------------------|------------------|--------|
|              |                            | $q_{1, \text{cal}}$ (mg/g) | $k_1$ (1/min) | $R_1^2$ | $q_{2, \text{cal}}$ (mg/g) | $K_2$ (g/mg min) | $R^2$  |
| 10           | 0.8                        | 1.92575                    | 0.010133      | 0.8927  | 0.770951                   | 0.076126         | 0.9979 |
| 25           | 1.8                        | 1.272038                   | 0.013588      | 0.9476  | 1.865672                   | 0.025619         | 0.9934 |
| 50           | 4                          | 3.755779                   | 0.013588      | 0.9558  | 3.520654                   | 0.014904         | 0.995  |
| 75           | 5                          | 2.760578                   | 0.007139      | 0.8435  | 5.277045                   | 0.007581         | 0.9912 |
| 100          | 6.5                        | 4.93401                    | 0.011745      | 0.9513  | 6.72495                    | 0.005382         | 0.9922 |

6.72 mg/g) calculated by pseudo-second-order equation were all close to those actually determined (0.8, 1.8, 4, 5 and 6.5) at the given concentration.

A similar result is reported for the removal of crystal violet on palm kernel fiber by El-Sayed [31], where the parameters and the adsorption capacity results suggested that the pseudo-second-order model has the best equation to represent the dye adsorption kinetics. Hameed et al. [49] employed sunflower seed (*Helianthus annuus* L.) hull for the removal of methyl violet from aqueous solutions. The pseudo-second-order model best described the sorption process. Olive pomace evaluated for the removal of reactive textile dye, RR198 by Akar et al. [50]. The sorption kinetics of the dye was well explained through pseudo-second-order kinetic model [50].

#### 4. Conclusion

The present study shows that the *Salvia sclarea* seeds (SSS) can be used as an adsorbent for the removal of basic violet 16 dyes from aqueous solutions. The SSS biosorbent demonstrated a high adsorption capacity in the adsorption of the BV 16 dye. The amount of dye sorbent was found to vary with increasing initial solution pH, and the maximum adsorption was observed at pH 7. The equilibrium was attained in 180 min. The amount of dye uptake (mg/g) increased from 0.701 to 15.625 mg/g in the concentration range of 10–300 mg/L. The removal percentage increased from 25.8% to 51.76% when the amount of the adsorbent was increased from 2.5 to 17.5 g after 60 min contact time. The kinetic studies of dye on the SSS were performed based

on the pseudo-first-order and pseudo-second-order. The data indicated that the adsorption kinetics of dye on the SSS followed the pseudo-second-order model at different dye concentrations. The experimental data have been analyzed using the Langmuir, Freundlich and Temkin isotherm models and the characteristic parameters for each isotherm were determined. The results showed that the experimental data were correlated reasonably well by the Langmuir isotherm. Based on the results of the present study, the *Salvia sclarea* seeds can be used as an eco-friendly adsorbent for the removal of dye from textile wastewater.

#### Acknowledgment

The authors would like to acknowledge Ardabil University of Medical Sciences (code: IR.ARUMS.REC.1396.184) for financial and instrumental supports.

#### References

- [1] J.-L. Gong, B. Wang, G.-M. Zeng, C.-P. Yang, C.-G. Niu, Q.-Y. Niu, W.-J. Zhou, Y. Liang, Removal of cationic dyes from aqueous solution using magnetic multi-wall carbon nanotube nanocomposite as adsorbent, *J. Hazard. Mater.*, 164 (2009) 1517–1522.
- [2] B. Shahmoradi, A. Maleki, K. Byrappa, Removal of Disperse Orange 25 using in situ surface-modified iron-doped TiO<sub>2</sub> nanoparticles, *Desal. Wat. Treat.*, 53 (2015) 3615–3622.
- [3] B. Shahmoradi, M. Pirsaeheb, M. Pordel, T. Khosravi, R.R. Pawar, S.-M. Lee, Photocatalytic performance of chromium-doped TiO<sub>2</sub> nanoparticles for degradation of reactive black 5 under natural sunlight illumination, *Desal. Wat. Treat.*, 67 (2017) 324–331.

- [4] T. Robinson, G. McMullan, R. Marchant, P. Nigam, Remediation of dyes in textile effluent: a critical review on current treatment technologies with a proposed alternative, *Bioresour. Technol.*, 77 (2001) 247–255.
- [5] O. Duman, S. Tunç, T.G. Polat, B.K. Bozoğlan, Synthesis of magnetic oxidized multiwalled carbon nanotube- $\kappa$ -carrageenan-Fe<sub>3</sub>O<sub>4</sub> nanocomposite adsorbent and its application in cationic Methylene Blue dye adsorption, *Carbohydr. Polym.*, 147 (2016) 79–88.
- [6] M. Naghizade Asl, N.M. Mahmodi, P. Teymouri, B. Shahmoradi, R. Rezaee, A. Maleki, Adsorption of organic dyes using copper oxide nanoparticles: isotherm and kinetic studies, *Desal. Wat. Treat.*, 57 (2016) 25278–25287.
- [7] Z. Rahmani, M. Kermani, M. Gholami, A.J. Jafari, N.M. Mahmoodi, Effectiveness of photochemical and sonochemical processes in degradation of Basic Violet 16 (BV16) dye from aqueous solutions, *Iran. J. Environ. Health Sci. Eng.*, 9 (2012) 14.
- [8] R. Jain, M. Mathur, S. Sikarwar, A. Mittal, Removal of the hazardous dye rhodamine B through photocatalytic and adsorption treatments, *J. Environ. Manage.*, 85 (2007) 956–964.
- [9] P. Manikandan, P. Palanisamy, R. Baskar, P. Sakthisharmila, Influence of Chemical Structure of Reactive Blue (Diazo), Direct Red (Diazo) and Acid Violet (Triaryl Alkane) Dyes on the Decolorization Efficiency by Photo Assisted Chemical Oxidation Process (PACO), *Int. J. Eng. Technol. Res.*, 5 (2017) 1–14.
- [10] A.R. Rahmani, A. Shabanloo, M. Fazlzadeh, Y. Poureshgh, Investigation of operational parameters influencing in treatment of dye from water by electro-Fenton process, *Desal. Wat. Treat.*, 57 (2016) 24387–24394.
- [11] G. Actis Grande, G. Rovero, S. Sicardi, M. Giansetti, Degradation of residual dyes in textile wastewater by ozone: comparison between mixed and bubble column reactors, *Can. J. Chem. Eng.*, 95 (2017) 297–306.
- [12] F. Abiri, N. Fallah, B. Bonakdarpour, Sequential anaerobic-aerobic biological treatment of colored wastewaters: case study of a textile dyeing factory wastewater, *Water Sci. Technol.*, 75 (2017) 1261–1269.
- [13] A. Othmani, A. Kesraoui, M. Seffen, The alternating and direct current effect on the elimination of cationic and anionic dye from aqueous solutions by electrocoagulation and coagulation flocculation, *Euro-Mediterr. J. Environ. Integr.*, 2 (2017) 6.
- [14] L. Yang, Z. Wang, J. Zhang, Zeolite imidazolate framework hybrid nanofiltration (NF) membranes with enhanced permselectivity for dye removal, *J. Membr. Sci.*, 532 (2017) 76–86.
- [15] L. Lakshmanraj, A. Gurusamy, M. Gobinath, R. Chandramohan, Studies on the biosorption of hexavalent chromium from aqueous solutions by using boiled mucilaginous seeds of *Ocimum americanum*, *J. Hazard. Mater.*, 169 (2009) 1141–1145.
- [16] K. Vikrant, B.S. Giri, N. Raza, K. Roy, K.-H. Kim, B.N. Rai, R.S. Singh, Recent advancements in bioremediation of dye: current status and challenges, *Bioresour. Technol.*, 253 (2018) 355–367.
- [17] M. Shirmardi, N. Alavi, E.C. Lima, A. Takdastan, A.H. Mahvi, A.A. Babaei, Removal of atrazine as an organic micro-pollutant from aqueous solutions: a comparative study, *Process Saf. Environ. Prot.*, 103 (2016) 23–35.
- [18] F.A. Pavan, E.S. Camacho, E.C. Lima, G.L. Dotto, V.T.A. Branco, S.L.P. Dias, Formosa papaya seed powder (FPSP): preparation, characterization and application as an alternative adsorbent for the removal of crystal violet from aqueous phase, *J. Environ. Chem. Eng.*, 2 (2014) 230–238.
- [19] R. Gong, S. Zhu, D. Zhang, J. Chen, S. Ni, R. Guan, Adsorption behavior of cationic dyes on citric acid esterifying wheat straw: kinetic and thermodynamic profile, *Desalination*, 230 (2008) 220–228.
- [20] S.M.A. Razavi, S.W. Cui, Q. Guo, H. Ding, Some physicochemical properties of sage (*Salvia macrosiphon*) seed gum, *Food Hydrocolloids*, 35 (2014) 453–462.
- [21] S.M.A. Razavi, A. Bostan, R. Rahbari, Computer image analysis and physico-mechanical properties of wild sage seed (*Salvia macrosiphon*), *Int. J. Food Prop.*, 13 (2010) 308–316.
- [22] J.-R. Jeon, E.-J. Kim, Y.-M. Kim, K. Murugesan, J.-H. Kim, Y.-S. Chang, Use of grape seed and its natural polyphenol extracts as a natural organic coagulant for removal of cationic dyes, *Chemosphere*, 77 (2009) 1090–1098.
- [23] A. Takdastan, A.H. Mahvi, E.C. Lima, M. Shirmardi, A.A. Babaei, G. Goudarzi, A. Neisi, M. Heidari Farsani, M. Vosoughi, Preparation, characterization, and application of activated carbon from low-cost material for the adsorption of tetracycline antibiotic from aqueous solutions, *Water Sci. Technol.*, 74 (2016) 2349–2363.
- [24] A.A. Babaei, E.C. Lima, A. Takdastan, N. Alavi, G. Goudarzi, M. Vosoughi, G. Hassani, M. Shirmardi, Removal of tetracycline antibiotic from contaminated water media by multi-walled carbon nanotubes: operational variables, kinetics, and equilibrium studies, *Water Sci. Technol.*, 74 (2016) 1202–1216.
- [25] M. Haghighi, F. Rahmani, R. Dehghani, A.M. Tehrani, M.B. Miranzadeh, Photocatalytic reduction of Cr (VI) in aqueous solution over ZnO/HZSM-5 nanocomposite: optimization of ZnO loading and process conditions, *Desal. Water Treat.*, 58 (2017) 168–180.
- [26] M.V. Niri, A.H. Mahvi, M. Alimohammadi, M. Shirmardi, H. Golastanifar, M.J. Mohammadi, A. Naeimabadi, M. Khishdost, Removal of natural organic matter (NOM) from an aqueous solution by NaCl and surfactant-modified clinoptilolite, *J. Water Health.*, 13 (2015) 394–405.
- [27] M.O. Borna, M. Pirsaeheb, M.V. Niri, R.K. Mashizie, B. Kakavandi, M.R. Zare, A. Asadi, Batch and column studies for the adsorption of chromium (VI) on low-cost Hibiscus *Cannabinus kenaf*, a green adsorbent, *J. Taiwan Inst. Chem. Eng.*, 68 (2016) 80–89.
- [28] Y. Rashtbari, S. Hazrati, S. Afshin, M. Fazlzadeh, M. Vosoughi, Data on cephalixin removal using powdered activated carbon (PPAC) derived from pomegranate peel, *Data in Brief*, 20 (2018) 1434–1439.
- [29] S. Afshin, S.A. Mokhtari, M. Vosoughi, H. Sadeghi, Y. Rashtbari, Data of adsorption of Basic Blue 41 dye from aqueous solutions by activated carbon prepared from filamentous algae, *Data in Brief*, 21 (2018) 1008–1013.
- [30] Y. Ho, G. McKay, The kinetics of sorption of basic dyes from aqueous solution by sphagnum moss peat, *Can. J. Chem. Eng.*, 76 (1998) 822–827.
- [31] G.O. El-Sayed, Removal of methylene blue and crystal violet from aqueous solutions by palm kernel fiber, *Desalination*, 272 (2011) 225–232.
- [32] K. Nadafi, M. Vosoughi, A. Asadi, M.O. Borna, M. Shirmardi, Reactive Red 120 dye removal from aqueous solution by adsorption on nano-alumina, *J. Water Chem. Technol.*, 36 (2014) 125–133.
- [33] H. Golestanifar, A. Asadi, A. Alinezhad, B. Haybati, M. Vosoughi, Isotherm and kinetic studies on the adsorption of nitrate onto nanoalumina and iron-modified pumice, *Desal. Wat. Treat.*, 57 (2016) 5480–5487.
- [34] H. Biglari, S. RodriguezCouto, Y.O. Khaniabadi, H. Nourmoradi, M. Khoshgoftar, A. Amrane, M. Vosoughi, S. Esmaeili, R. Heydari, M.J. Mohammadi, Cationic surfactant-modified clay as an adsorbent for the removal of synthetic dyes from aqueous solutions, *Int. J. Chem. Reactor Eng.*, 16 (2018) 342–356.
- [35] N.M. Mahmoodi, B. Hayati, M. Arami, Kinetic, equilibrium and thermodynamic studies of ternary system dye removal using a biopolymer, *Ind. Crops Prod.*, 35 (2012) 295–301.
- [36] A.S. Sartape, A.M. Mandhare, V.V. Jadhav, P.D. Raut, M.A. Anuse, S.S. Kolekar, Removal of malachite green dye from aqueous solution with adsorption technique using *Limonia acidissima* (wood apple) shell as low cost adsorbent, *Arabian J. Chem.*, 10 (2017) S3229–S3238.
- [37] R. Katal, M.V. Sefti, M. Jafari, A.H.S. Dehaghani, S. Sharifian, M.A. Ghayyem, Study effect of different parameters on the sulphate sorption onto nano alumina, *J. Ind. Eng. Chem.*, 18 (2012) 230–236.
- [38] V. Gupta, B. Gupta, A. Rastogi, S. Agarwal, A. Nayak, A comparative investigation on adsorption performances of mesoporous activated carbon prepared from waste rubber tire and activated carbon for a hazardous azo dye Acid Blue 113, *J. Hazard. Mater.*, 186 (2011) 891–901.

- [39] M.C.S. Reddy, L. Sivaramakrishna, A.V. Reddy, The use of an agricultural waste material, Jujuba seeds for the removal of anionic dye (Congo red) from aqueous medium, *J. Hazard. Mater.*, 203 (2012) 118–127.
- [40] R. Katal, S. Pourkarimi, E. Bahmani, H.A. Dehkordi, M.A. Ghayyem, H. Esfandian, Synthesis of Fe<sub>3</sub>O<sub>4</sub>/polyaniline nanocomposite and its application for nitrate removal from aqueous solutions, *J. Vinyl Add. Tech.*, 19 (2013) 147–156.
- [41] W.-h. Xu, G. Zhang, S.-c. Zou, X.-d. Li, Y.-c. Liu, Determination of selected antibiotics in the Victoria Harbour and the Pearl River, South China using high-performance liquid chromatography-electrospray ionization tandem mass spectrometry, *Environ. Pollut.*, 145 (2007) 672–679.
- [42] I.A.W. Tan, A.L. Ahmad, B.H. Hameed, Adsorption of basic dye on high-surface-area activated carbon prepared from coconut husk: equilibrium, kinetic and thermodynamic studies, *J. Hazard. Mater.*, 154 (2008) 337–346.
- [43] J.F. Osmá, V. Saravia, J.L. Toca-Herrera, S.R. Couto, Sunflower seed shells: a novel and effective low-cost adsorbent for the removal of the diazo dye Reactive Black 5 from aqueous solutions, *J. Hazard. Mater.*, 147 (2007) 900–905.
- [44] D. Chakraborty, S. Maji, A. Bandyopadhyay, S. Basu, Biosorption of cesium-137 and strontium-90 by mucilaginous seeds of *Ocimum basilicum*, *Bioresour. Technol.*, 98 (2007) 2949–2952.
- [45] S. Khattri, M. Singh, Removal of malachite green from dye wastewater using neem sawdust by adsorption, *J. Hazard. Mater.*, 167 (2009) 1089–1094.
- [46] C.P. Sekhar, S. Kalidhasan, V. Rajesh, N. Rajesh, Bio-polymer adsorbent for the removal of malachite green from aqueous solution, *Chemosphere.*, 77 (2009) 842–847.
- [47] C. Namasivayam, K. Kadirvelu, Coirpith, an agricultural waste by-product, for the treatment of dyeing wastewater, *Bioresour. Technol.*, 48 (1994) 79–81.
- [48] S.D. Khattri, M.K. Singh, Colour removal from dye wastewater using sugar cane dust as an adsorbent, *Adsorpt. Sci. Technol.*, 17 (1999) 269–282.
- [49] B. Hameed, Equilibrium and kinetic studies of methyl violet sorption by agricultural waste, *J. Hazard. Mater.*, 154 (2008) 204–212.
- [50] T. Akar, I. Tosun, Z. Kaynak, E. Ozkara, O. Yeni, E.N. Sahin, S.T. Akar, An attractive agro-industrial by-product in environmental cleanup: dye biosorption potential of untreated olive pomace, *J. Hazard. Mater.*, 166 (2009) 1217–1225.